

Role of Xalas2 in Regulating Erythroblast Differentiation during Primary Hematopoiesis in *Xenopus laevis*

著者	小川 朝子
year	2016
その他のタイトル	アフリカツメガエル一次造血期の赤芽球分化を制御するXalas2遺伝子の役割
学位授与大学	筑波大学 (University of Tsukuba)
学位授与年度	2015
報告番号	12102甲第7741号
URL	http://hdl.handle.net/2241/00143894

**Role of *Xalas2* in Regulating Erythroblast Differentiation
during Primary Hematopoiesis in *Xenopus laevis***

A Dissertation Submitted to

the Graduate School of Life and Environmental Sciences,

the University of Tsukuba

in Partial Fulfillment of the Requirements

for the degree of Doctor of Philosophy in Biological Science

(Doctoral Program in Biological Sciences)

Asako OGATA-OTOMO

Table of contents

Table of contentsii
I. Abstract1
II. Abbreviations3
III. Introduction6
III-1. <i>The mechanism of erythrocytosis</i>	
III-2. <i>The role of Alas2 in vertebrate erythrocytosis</i>	
III-3. <i>Objective of this study</i>	
IV. Materials and methods.....	14
IV-1. <i>Animals</i>	
IV-2. <i>Embryo culture and manipulation</i>	
IV-3. <i>RNA extraction and RT-PCR</i>	
IV-4. <i>RNA synthesis in vitro</i>	

IV-5. *Explant culture*

IV-6. *DNA microarray*

IV-7. *MO design and activities*

IV-8. *Whole-mount in situ hybridization (WISH)*

IV-9. *Hemoglobin staining for and transparent cleaning*

IV-10. *Collection of peripheral blood from larva and Giemsa staining*

V. Results24

V-1. *Alignment of Xalas2*

V-2. *Xalas2 expression*

V-3. *Translational inhibition of Xalas2 leads to the loss of hemoglobin*

V-4. *XAlas2 affects differentiation of erythroblast*

V-5. *Xalas2 regulated hba3 expression*

V-6. *Xalas2 is required for the proliferation or/and differentiation of*

erythroblast

VI. Discussion	32
VII. Acknowledgements	38
VIII. Reference	37
IX. Legends and Figures	47

I. Abstract

In adult vertebrates, all blood cells originate from hematopoietic stem cells, produced from hemangioblasts at the fetal stage. The hemangioblast, located within the yolk sac in the embryo, produces hematopoietic stem cells, early erythroblasts, macrophages, and vascular endothelial cells by a process called as primary hematopoiesis. Subsequently, hematopoietic stem cells are generated in the liver, allowing secondary hematopoiesis to continue even after achieving adulthood. During primary hematopoiesis in mammals, birds, amphibians, and teleost fishes, major transcription factors such as GATA1, GATA2, and SCL are expressed in the hemangioblast. Fetal-type globin genes, which are the targets of these transcription factors, are expressed during erythroblast differentiation. However, the mechanisms by which hemangioblasts specifically differentiate into erythroblasts during primary hematopoiesis are unclear. I selected the *Xenopus laevis* model due to the ease in inducing organ formation to identify specific genes whose time-specific expression would allow differentiation between hemangioblasts and erythroblasts. I identified a heme synthetase, aminolevulinic acid synthase gene (*alas2*). In this study, I investigated

the function of *Xenopus alas2* (*Xalas2*) and showed that *Xalas2* mediated erythroblast differentiation in primary hematopoiesis by regulating *hba3* expression.

II. Abbreviations

ALAS: aminolevulinic acid synthase

aVBI: anterior VBI

BB/BA: benzylbenzoate / benzyl alcohol

BFU-E: erythroid burst-forming units

BSA: Bovine serum albumin

DHS: DnaseI hypersensitive site

DLP: dorsal lateral plate

CFU-E: erythroid colony-forming units

DNA: deoxyribonucleic acid

EDTA: ethylenediaminetetraacetic acid

EGFP: enhanced green fluorescent protein

EGTA: ethylene glycol tetra acetic acid

FBS: fetal bovine serum

hba 3: α -globin 3

HRP: horseradish peroxidase

IL: interleukin

IGF-1: insulin-like growth factor-1

IRE: iron-responsive element

IRP: IRE-binding protein

KLF1: kruppel-like factor 1

MBSH: 1×high-salt modified Barth's saline

MEMFA: magnesium sulfate/formaldehyde buffer

MO: antisense morpholino oligonucleotide

MT: myc taq

NF-E2: nuclear factor erythroid-derived 2

OCD: ornithine decarboxylase

pVBI: posterior VBI

PVDF: Polyvinylidene DiFluoride

RACE: Rapid Amplification of cDNA Ends

RNA: ribonucleotic acid

RT-PCR: reverse transcription-polymerase chain reaction

SCL: stem cell leukemia

SDS-PAGE: sodium dodecyl sulfate -polyacrylamide gel electrophoresis

TBST: Tris-buffered saline with Tween[®] 20

UTR: untranslated region

VBI: ventral blood island

VMZ: ventral marginal zone

WISH: whole mount in situ hybridization

X. laevis: *Xenopus laevis*

Xalas2: *Xenopus* delta-aminolevullnate synthase 2

III. Introduction

III-1. *The mechanism of erythrocytosis*

Vertebrate hematopoietic development consists of two phases: primitive and definitive. In mice, progenitors of the primitive erythrocyte lineage arise from the mesoderm during gastrulation in the yolk sac region, called the blood island (Palis et al 2001), (Baron et al 2013). Subsequently, definitive hematopoiesis involving the production of primitive erythrocytes occurs first in the aorta-gonad-mesonephros, second in the placenta during embryogenesis, and finally in the fetal liver (Tsiftoglou et al 2009). Primitive hematopoiesis results in the formation of erythroblasts, megakaryocytes, and macrophages in the yolk sac (Tober et al 2007). The nuclei and hemoglobin of these erythroblasts are comprised of a heterotetramer of two α - and β -subunits of globin-containing heme (Palis et al 2014). At this stage, the β -subunit globin exists in the fetal form, $\epsilon\gamma$ -globin (Wilber et al 2011). Enucleated erythrocytes are produced at the definitive hematopoiesis stage in the fetal liver. After birth, β -subunit hemoglobin of the adult type is produced in enucleated erythrocytes within the bone marrow (Tsiftoglou et al 2009).

The developmental mechanism differs between primitive and definitive erythrocytes. In the mouse, cytokines including interleukin (IL)-3, stem cell leukemia (SCL), and insulin-like growth factor-1 (IGF-1) act on hematopoietic stem cells during definitive hematopoiesis. These cells differentiate into erythroid burst-forming units (BFU-E), which express transcription factors Pu.1, GATA2, and SCL. Subsequently, erythropoietin specifically causes not only differentiation into erythroid colony-forming units (CFU-E) but also proliferation. CFU-E, expressing GATA1, GATA2, SCL, Sox6, nuclear factor erythroid-derived 2 (NF-E2), and kruppel-like factor 1 (KLF1) differentiate into pro-erythrocytes (Baron 2013). In contrast, erythroblast progenitors express fetal liver kinase 1 (Flk1), c-kit, Etv2, SCL, vascular endothelial (VE)-cadherin, and Tie2 during primitive hematopoiesis (Baron 2013). These cells have the ability to differentiate into both, endothelial, or hematopoietic cells. Furthermore, erythroblast progenitors also express adhesion proteins on their surface, such as CD44 (hyaluronan receptor) and integrins $\alpha 4$, $\alpha 5$, and $\beta 1$ in the yolk sac (Isern et al 2011). In fact, tight associations within erythroblast progenitors have been observed in the yolk sac using electron microscopy (Haar and Ackerman 1971). Expression of these adhesion proteins

and increase in metalloprotease expression were lost before entering into blood vessel.

However, the mechanism of hemangioblast differentiation into erythroblasts in terms of signal pathways before entering the bloodstream is unclear.

III-2. *The role of ALAS2 in vertebrate erythrocytosis*

In vertebrates, the main function of the erythrocyte involves transport of oxygen via hemoglobin. Hemoglobin consists of a heterotetramer of two α - and β -subunits of globin carrying a synthesized heme complex, consisting of divalent iron (FeII) and porphyrin. However, heme also regulates several biological processes through heme-responsive or heme-sensitive proteins (Sun et al 2004). Heme controls erythrocyte differentiation independently as a transcriptional regulator with the exception of forming a complex with globin protein. For example, heme-regulated eIF2 α kinase regulates translational initiation in diverse stress conditions by phosphorylation of the α -subunit of eIF2, activation of Atf4 signaling pathway in reducing oxidative stress, and in erythropoiesis (Rajeasekhar et al 2012). In addition, heme-mediated transcriptional activation of heme oxygenase-1 and globin gene through transcription repressor Bach1 in murine erythroleukemia cells (Furuyama et al 2007).

The detailed mechanism of hemoglobin synthesis in the mammalian erythrocytes has been studied previously. The heme synthesis pathway is evolutionarily conserved in vertebrates (Ajioka et al 2006). Two aminolevulinic acid synthase (ALAS) isozymes are encoded by *ALAS-1* (also known as non-specific ALAS), which is nonspecifically expressed in adult mammals, and *ALAS-2* (also known as erythroid ALAS), which is specifically expressed in erythroid cells (Riddle et al 1989). In the mouse, *Alas2* transcription is regulated by iron and iron-related proteins. *Alas2* 5'-untranslated region (UTR) contains an iron-responsive element (IRE; 5-CAGUGX-3) (Melefors et al 1993) similar to that found in man, mouse, rat, and chicken. IRE-binding protein (IRP) binds to IRE-sequences in *ALAS2* (Kim et al 1996). *Alas2* translation is inhibited by forming of a stem-loop structure with IRE under conditions of low iron concentration. In the presence of high iron concentration, iron forms complexes with IRP and inactivates it, therefore IRP does not bind to IRE. The translated *Alas2* moves from the cytosol to mitochondria and the pre-sequence including mitochondria transport signal is cleaved by ALAS to release the mature protein enzyme δ -ALA, followed by a catalytic series that leads to the formation of heme. This catalytic series is mediated by

ALA dehydratase, porphobilinogen deaminase, uroporphyrinogen III synthase, uroporphyrinogen decarboxylase, coproporphyrinogen oxidase, protoporphyrinogen oxidase, and ferrochelatase in the mitochondria and cytosol. ALAS2 is essential for heme synthesis in erythrocytes and deletion of the C-terminal of ALAS2 causes X-linked dominant protoporphyria in humans.

Few *in vivo* studies have been reported regarding the function of *Alas2* in developmental biology, especially during primary hematopoiesis, which occurs in the yolk sac in vertebrates. *Alas2*-knockout mice exhibited formation of abnormal erythrocytes, accumulation of iron, and decrease in globin protein at embryonic day 10.5 (E10.5), resulting in death due to anemia at E11.5 caused by defective hemoglobin (Nakajima et al 1999). These data demonstrated the role of *Alas2* function in erythrocyte production during both, primary and definitive hematopoiesis. In a study in zebrafish, reduction of hemoglobin was confirmed by staining with o-dianisidine in case of mutations in *sauternes (sau)* gene, orthologue of mouse *Alas2*. Additionally, erythroblasts generated by definitive hematopoiesis were immature (Beownlie et al

1998). However, the role of ALAS2 in erythroblast differentiation in vertebrates during primary hematopoiesis is unknown.

Xenopus (frog), chicken, and quail are frequently used as hematopoiesis models because of species-specific advantages. *Xenopus laevis* is particularly useful for large-scale screening and functional analyses. Eggs are available year-round and artificial fertilization is easy to perform. In addition, extensive information regarding *Xenopus* cleavage patterns and fate map is available. Moreover, the transparent tadpole is suitable for observation of blood cells. Primitive hematopoiesis in *X. laevis* begins at the neurula-stage mesoderm in the ventral blood island (VBI). The primitive VBI expresses hematopoietic and endothelial markers, Flk-1, Fli-1, and Gata2 at the neurula stage, comparable to the hemangioblast in mammals. The VBI, equivalent to the yolk sac blood island of amniotes, produces a primitive erythroblast, which is released for circulation into peripheral blood vessels through the vitelline vein. VBIs have discernable anterior and posterior regions. Progenitors of the anterior VBI (aVBI) are derived from the dorsal marginal zone, while those of posterior VBI (pVBI) are derived from the ventral marginal zone (Ciau-Uitz et al 2000). Myeloid genes such as *SpiB* and

Mpo are expressed in aVBI, whereas erythroid genes such as *Runx*, *Lmo2*, and *Scl (tal1)* are expressed in pVBI during the neurula stage (Costa et al 2000 and Walmsley et al 2008). The erythroblast progenitors in pVBI express the mature marker, larval globin. However, the mechanism of differentiation into mature erythrocytes with respect to the signal pathway, before entering the bloodstream remains unknown.

In this study, I explored whether ALAS2 has functions other than heme synthesis in primitive hematopoiesis based on heme transcription regulation. I showed that *Xenopus alas2 (Xalas2)* is first expressed in primitive erythroblast during primary hematopoiesis before transcription of embryonic globin. Moreover, by comparing the effect of synthesis inhibitor with *Xalas2* translational inhibition, I demonstrate that *Xalas2* independently controls the differentiation of erythroblast in primitive hematopoiesis via a heme-mediated independent mechanism.

III-3. *Objective of this study*

The mechanism of hemangioblast differentiation into mature erythrocytes with respect to the signal pathway, before entering the bloodstream is currently unknown. Using *Xenopus laevis* as model organism, I identified *Xalas2*, a gene with time-specific expression that allows for distinction between hemangioblasts and erythroblasts. The purpose of this study was to determine the role of *Xalas2* in erythroblast differentiation during primary hematopoiesis.

IV. Materials and methods

IV-1. *Animals*

This study was conducted in accordance with the Guideline for Proper Conduct of Animal Experiments by the Science Council of Japan. All experiments were performed at the National Institute of Advanced Industrial Science and Technology between 2012 and 2015.

IV-2. *Embryo culture and manipulation*

The adult frogs (*X. laevis*) of both sexes, were purchased from Watanabe Zoushoku and Hamamatsu Seibutsu Kyouzai. Adult female frogs were maintained in an incubator (Panasonic) at 21°C-23°C for approximately more than 13 hr after being injected with 100 U/ml human chorionic gonadotropin (Gestron; Kyoritsu Seiyaku) to obtain eggs. On the same day, adult male frogs were placed in ice-cold water to simulate a semi-hibernation state and testes were collected. The testes were stored in fetal bovine serum (FBS; Millipore) containing 10% Steinberg's solution (17% NaCl, 0.5% KCl, 0.5% CaCl₂, and 1.025% MgSO₄) at 4°C until use. A fresh suspension of

sperm was prepared by mincing testes in De Boer's solution (0.11 M NaCl, 0.0013 M KCl, 0.00044 M CaCl₂ NaHCO₃) immediately before fertilization. Eggs were obtained from the cloaca of the injected female frog by applying pressure ventrally. The eggs were mixed with sperm in a petri dish and left standing for 6 min at RT for fertilization. Fertilized eggs were cultured in 0.5% De Boer's solution. Subsequently, the embryos were de-jellied using 1% sodium thioglycollate (Tashiro et al 1999) and washed several times with 10% Steinberg's solution. The embryos were then injected with each nucleotide in 1× high-salt, modified Barth's saline (MBSH)/5% Ficoll. The culture medium of the embryos was replaced with 10% Steinberg's solution before gastrulation.

IV-3. RNA extraction and reverse transcription-polymerase chain reaction (RT-PCR)

Total RNA was extracted from embryos and adult organs using phenol method as previously described (Ito et al 2001). Briefly, embryos or organs frozen under liquid nitrogen were crushed in homogenization solution (100 mM Tris-Cl, 50 mM NaCl, 10 mM ethylenediaminetetraacetic acid [EDTA], and 0.5% sodium dodecyl sulfate [SDS]), supplemented with 20 mg/ml Proteinase K (Sigma-Aldrich), followed by incubation at 37°C for 1 hr. The solution was extracted with phenol/chloroform

(TE-saturated), followed by chloroform and 5 M ammonium acetate was added to the aqueous phase. The mixture was stored at 0°C and centrifuged for 20 min.

Nuclease-free water, 3 M ammonium acetate (pH 5.2), and 100% ethanol was added to the RNA extract, centrifuged, and rinsed with 70% ethanol. First-strand cDNA was synthesized from extracted total RNA using an oligo-(dT) primer and SuperScript™ III RT (Life Technologies). The resulting cDNA was used as a template for reverse transcription-polymerase chain reaction (RT-PCR). Ornithine decarboxylase (*ODC*) gene was used as a positive control. For cloning of various globin cDNA, sequence information for globin primers were obtained from Xenbase genome database (<http://www.xenbase.org/entry/>). RT-PCR was performed using KOD-plus-neo kit (Toyobo) as described in manufacture instructions. The amplified globin cDNA were cloned into pBluescript II SK+ vector and sequences were analyzed by 3500 Genetic Analyzer (Thermo Fisher) to identify high-homology sequence of each gene. All primer sequences used for cloning are listed in Table 1.

IV-4. *RNA synthesis in vitro.*

The clones of *Xalas2* mRNA (accession No: BC080015) and RhoBTB mRNA

(NM_001092210) were purchased from Thermo Fisher Scientific K.K (Open Biosystems). These sequences were sub-cloned in pCS2 vectors. The plasmids PCS2 dkk1, pCS2 EGFP, and pCS2 Red-gal were obtained from Dr. Asashima. These plasmids were digested with *Not I* (Takara), and capped RNA was synthesized using mMESSAGE mMACHINE[®] SP6 Kit (Life Technologies). After synthesis and DNase I treatment, 20 µl RNA solution was mixed with 250 µl nuclease-free water and 30 µl ammonium acetate (3 M, pH 5.2), and extracted with phenol/chloroform (Tris-EDTA-saturated), followed by extraction with chloroform. The aqueous layer of the extract was mixed with 1 volume isopropanol and centrifuged. Precipitated RNA was rinsed in 70% ethanol and purified by repeating isopropanol precipitation. Quality of the synthesized RNA was confirmed by gel electrophoresis and concentration of RNA was measured at 260 nm absorbance using a Nano Drop (Thermo Fisher).

IV-5. Explant culture

The embryos injected with messenger RNA (mRNA) were cultured up to Stage 10. The ventral marginal zone (VMZ) of the embryo was cut using a tungsten-needle in MBSH/1% bovine serum albumin (BSA) solution. The VMZ were

cultured with MBSH/1% BSA supplemented with 4-Methylumbelliferone until Stage 23 and then frozen under liquid nitrogen.

IV-6. *DNA microarray*

Total RNA was isolated using the same method from each VMZ as IV-5. Complementary cRNA was synthesized from total RNA, labeled with Cy3-dye, and microarray analysis was conducted using *Xenopus* Oligo microarrays (G2514F, Agilent). Each sample was hybridized with one-color protocol and fluorescence signals were detected using a G2514F microarray scanner system (Agilent). These data were analyzed by GeneSpring GX10 software (Agilent).

IV-7. *MO design and activities*

I identified *Xalas2* 5'-UTR sequence by 5' rapid amplification of cDNA ends using SMARTerTM Rapid Amplification of cDNA Ends (RACE) cDNA Amplification Kit (Clontech), *Xalas2*-morpholino antisense oligonucleotide (*xalas2*-MO) was designed as described by Gene Tools, LLC (<https://store.gene-tools.com>). MO sequences were as follows: *Xalas2a*-MO,

5'-ACGATTAATGAGAGAAGCCATGTTC-3', and *Xalas2b*-MO, 5'-CAACGATTGATGAGAGAAGCCATGT-3'. I amplified *Xalas2* coding sequence with 5'-UTR or 5 point-mutations in the morpholino binding site by RT-PCR with high-fidelity DNA polymerase, *Pfu* (Promega), using primers listed in Table 2. The amplified fragments were digested with *Bam*HI and *Cla*I, and subcloned into the *Bam*HI and *Cla*I sites of the pCS2+MT vector. Two types of *Xalas2* RNA were synthesized *in vitro* using pCS2-5'-UTR-*Xalas2*-5myc and pCS2-5mis-*Xalas2*-5myc. To confirm the specificities of the MO, 2-cell stage embryos were injected with RNA and MOs, embryos were collected at Stage 9, and frozen in liquid nitrogen. The proteins of these embryos were extracted and separated by sodium dodecyl sulfate-polyacrylamide gel electrophoresis (SDS-PAGE). The proteins were transferred to PVDF membranes using iBlot dry blotting system (Life Technologies), and blocked with 10% skim milk (Nacalai Tesque) in Tris-buffered saline with Tween 20 (TBST) buffer (20 mM Tris-HCl [pH 7.6], 150 mM NaCl, and 0.05% Tween 20) overnight at 4°C. The membranes were incubated with SC-40 HRP-conjugated, Myc (19E10), mouse monoclonal antibody (Santa Cruz) diluted at 3000-fold in 10% skim milk/TBST

for 1 hr at room temperature, the membrane were washed 4 times with TBST and incubated with enhanced chemiluminescent assay reagent, SuperSignal West Femto (Pierce). The protein bands were visualized using an LAS1500 Analyzer (Fuji Film). The antibody was stripped from the membrane using stripping buffer (100 mM 2-mercaptoethanol, 2% SDS, 62.5 mM Tris-Cl [pH 6.7]). The membranes were re-probed with monoclonal anti-actin clone antibody AC-40 (Sigma Aldrich) as loading control diluted at 3000-fold in 10% skim milk/TBST for 1 hr at room temperature. The membranes were washed three times and probed with horseradish peroxidase (HRP)-conjugated anti-mouse IgG (H&L) antibody (Cell Signaling) diluted at 3000-fold as secondary antibody for 1 hr. The membranes were washed several times, visualized as described above.

IV-8. *Whole-mount in situ hybridization (WISH)*

The plasmids, pCMV-Sport6/*Xalas2*, pCMV-Sport6/*RhoBTB*, pGEM-T easy *hba3* (NM_001086328), pGEM-T *Gata1* (NM_001085640), pGEM-T *Gata2* (NM_001090574), and pBluescript II Sk-/*SCL* (Inui et al 2006) (NM_001088277 NM_001088278) were digested with restriction enzymes, as listed in Table 3. All

probes were synthesized using DIG RNA Labeling Mix (Roche), as listed in Table 3.

The embryos were processed for whole-mount *in situ* hybridization as previously described (Harland 1991); some embryos were embedded in paraffin, cut into 10- μ m sections, and stained with eosin.

IV-9. Hemoglobin staining and transparent clearing

Whole-embryo staining for heme expression was performed using o-dianisidine (Sigma Aldrich) histochemistry as previously described (Detrich et al 1995). After staining, the embryos were fixed in MOPS/EGTA/MEMFA for 3 hr and incubated in BB/BA for a few days.

IV-10. Collection of peripheral blood from larvae and Giemsa staining

The larva tails at Stage 42 were cut in 10% Steinberg's solution containing 0.5% BSA and 10 IU/ml heparin (Devorah et al 2006). Peripheral blood was collected into tubes and centrifuged at 2,000 rpm at room temperature for 10 min. Concentrated blood cells were smeared onto a slide, fixed with 100% methanol for a few minutes after drying, and stained with Giemsa solution (Wako) as per manufacturer instructions.

Table 1: Primer sequence for RT-PCR

Gene	Primer sequence
<i>Xalas2a</i>	Fw: 5'-ATCTTCACAACAAGGATGCA-3' Rv: 5'-GTTATATTGGGAAAGGAGGAC-3'
<i>Xalas2b</i>	Fw: 5'-GCCTGAAGAAGAAATTTCTAG-3' Rv: 5'-AAAGCAGGAGGAGAAAAGAAG-3'
<i>ODC</i>	Fw: 5'-GTCAATGATGGAGTGTATGGATC-3' Rv: 5'-TCCAATCCGCTCTCCTGAGCAC-3'

Table 2: Primer sequence for MO design and activities

Gene name	Primer sequence
Injected <i>Xalas2a</i>	Fw:5'-CCGGATCCAGTGCAGGGCAACAGAAAC-3'
	Rv:5'-CCATCGATCAGAGGCATACATAGTAATGTATTTT-3'
Injected <i>Xalas2a</i>	Fw:5'-CCGGATCCATGGCATCACTGATAAATCGATGTCCC-3'
	Rv:5'-CCATCGATCAGAGGCATACATAGTAATGTATTTT-3'
Injected <i>Xalas2b</i>	Fw:5'-CTTGACGTGTGAACATGGCTTCTCTCATCAATCG-3'
	Rv:5'-GTGTCTGTTGCCCTGCACTG-3'
Injected <i>Xalas2b</i>	Fw:5'-CCGGATCCATGGCATCACTGATAAATCGATGTCCC-3'
	Rv:5'-CCATCGATCAGAGGCATACATAGTAATGTATTTT-3'

Table 3: Details of WISH probes

Gene name	Restriction enzymes	RNA polymerase	Length (bp)
<i>Xalas2</i>	NotI	T7	2529
<i>RhoBTB</i>	SmaI	T7	4499
<i>hba3</i>	SpeI	T7	202
<i>Gata1</i>	EcoRI	T7	1080
<i>Gata2</i>	XbaI	T7	1362
<i>Scl</i>	SacII	T3	762

V. Results

V-1. Alignment of *Xalas2*

I cloned 5'-UTR sequences by RACE method and determined the coding sequence for *Xalas2*. The amino acid sequence was compared with that of other vertebrates. *Xalas2* contains 2 heme-regulatory motifs (CP motif: [Arg, Lys, or Asn]-Cys-Pro-[Lys or hydrophobic residue]-[Lue or Met]) (Figure 1). CP motifs in the mitochondrial pre-sequence of ALAS-1 and ALAS-2 proteins have been reported to bind heme (Furuyama et al 2007). Furthermore, pre-sequences contain a signal that targets mitochondria in mammalian species (Furuyama et al 2007), but quite different from those found in aquatic animals (Figure 1). The green arrowhead indicates the processing site of precursor protein by peptidase (Lathrop et al 1993), and the blue square shows the catalytic region for synthesis of 5-aminolevulinic acid from glycine and succinyl coenzyme A (Figure 1). This region in *X. laevis* shows homology with these of human, mouse, and zebrafish.

V-2. *Xalas2* expression

Firstly, *Xalas2* expression during early developmental stages was investigated using RT-PCR. The *Xalas2a* mRNA expression was detected from Stage 15, continuously induced until Stage 34, and maintained its level until Stage 42. Compared with *Xalas2a*, *Xalas2b* began to be expressed after Stage 38, when pro-erythrocytes entered circulation (Figure 2A). To analyze the spatiotemporal expression of *Xalas2*, I performed whole mount *in situ* hybridization. *Xalas2a* was expressed in anterior mesoderm at the neurula stage (Figure 2B, C). This expression was very similar to that of transcription factor, *Scl* (Figure 2K). SCL forms a transcriptional complex with E47, Lbd/NL1, LMO2, and GATA-1 to regulate hematopoiesis factors (Wadman et al 1997) and acts in the early anterior mesoderm to activate hematopoietic stem cells in *Xenopus laevis* (Mead et al 1998). At Stage 23, it was clearly shown that *Xalas2a* expression pattern was similar to that of *Scl*, two crossing lines for cardiac mesoderm and hemangioblast at Stage 23 (Figure 2D, D', L). *Xalas2a* was continuously expressed in the VBI and disappeared from the anterior cardiac region at approximately the tailbud stage (Figure 2E, E'). These expression patterns were similar to those of *hba3* (Figure 2I), one of the globin genes observed in the VBI before the cells entered the circulation.

The expression of *Xalas2* at Stage 38 was observed in the aortic arc near the cardiac region and the liver (Figure 2F, F'). These results suggested that *Xalas2* was expressed in circulating pro-erythroblasts and erythroblasts within certain blood vessels at the tadpole stage. Interestingly,

V-3. Translational inhibition of Xalas2 leads to loss of hemoglobin

I inhibited *in vivo* translation of 2 types *Xalas2* using *Xalas2*-MO as designed in Figure 3A and 3B. The blastomere in dorsal vegetal at the 8-cell stage is committed to the fate of hemangioblast at Stage 23. In contrast, an erythroblast precursor in the aVBI region at Stage 34, will not undergo further development in these tissue cells (Figure 3A and 3B). Staining of hemoglobin in the embryos injected with this MO by o-dianisidine confirmed the function of *Xalas2* during heme synthesis in erythroblast precursors and erythroblasts, at Stages 34 and 42, respectively (Figure 5A). Hemoglobin was hardly observed in the embryo after *Xalas2* MO injection in the 8-cell ventral vegetal-side at both 23 and 34 Stages. In particular, very few blood cells were seen within the cardiac atrium and ventricle at Stage 42, as in Figure 5B, lower panel. On the other hand, in the embryos injected into the dorsal vegetal side, hemoglobin levels

within the heart were decreased, compared with the control MO injected embryo (Figure 5A, lower panel). I inhibited heme synthesis pathway using an alternate method to verify whether biosynthesis of heme itself caused reduction of hemoglobin *in vivo*. Since succinylacetone is structurally similar to aminolevulinic acid, addition of succinylacetone competitively inhibits porphobilinogen synthase-dependent conversion of heme synthesis (Figure 6A). I found that amount of hemoglobin complex was decreased with an increase in dose of succinylacetone (Figure 6B). Particularly, at 0.25 mM succinylacetone, hemoglobin complexes disappeared altogether, in the erythroblast precursors at Stage 34 (Figure 11B) and in the circulating erythroblasts at Stage 42 (Figure 6B). While the addition of more than 0.25 mM succinylacetone resulted in non-specific phenotypes including edema, loss of a few somites, convulsion, and embryonic death before gastrulation, the optimal concentration (0.25 mM) of succinylacetone also showed similar phenotypes, albeit to a lesser extent, in addition to loss of hemoglobin.

V-4. XAlas2 controls the differentiation of erythroblasts

Next, involvement of *Xalas2* in erythroblast differentiation was confirmed by knockdown of 2 types of *Xalas2*, MO1 and MO2, which were injected into 2 blastomeres at the dorsal-vegetal or ventral-vegetal side at the 8-cell stage. The expression of *Scl* in the hemangioblast in *Xalas2* MO-injected embryo was not affected, as that in the control MO-injected embryos at Stage 23 (Figure 7A and 7B, left panel). By contrast, the expression of *Scl* was decreased in the aortic arch in the embryo injected with *Xalas2* MO at the dorsal vegetal region at Stage 34 (Figure 7A). Additionally, *Scl* expression disappeared in pVBI in the ventral vegetal region (red arrow in Figure 7B). Regarding *hba3*, V-shaped expression was somewhat diminished at Stage 34 in the aVBI in the embryos injected with *Xalas2* MO on the dorsal side (Figure 8A and 9A). However, in the aVBI, there was no difference in *hba3* expression between the embryos injected with the control MO and *Xalas2* MO (Figure 9A). By contrast, after ventral vegetal injection, expression was greatly decreased in pVBI (Figure 8B and 9B), and the embryo with decreased in pVBI was observed at high frequency from 62% to 82% compared with the control MO injected-embryos from 0 to 17% (Figure 9B and 9C). Injection of *Xalas2* MO with *Xalas2/5mis* mRNA containing

5 point-mutations in the MO binding site, rescued the expression of *hba3* approximately by 44% (Figure 10). The expression of *Gata1* and *Gata2*, which are transcription factors responsible for globin genes (Deconinck et al 2000), was not affected by *Xalas2* MO injection at Stages 23 and 34 (Figure 7B). In summary, inhibition of *Xalas2* translation did not affect development of hemangioblast at Stage 23 but impeded differentiation of erythroblast precursors (Figure 7, 8, and 10). Inhibition of *Xalas2* caused down-regulation of *hba3* expression (Figure 8 and 10). These data suggest that *Xalas2* functions in erythrocyte precursors of pVBI to regulate expression of *hba3*.

V-5. Xalas2-regulated hba3 expression

Next, I asked whether heme synthesized by *Xalas2* causes downregulation of *hba3* genes, I investigated the *hba3* expression pattern in embryos treated with succinylacetone at Stage 34 (Figure 11A). The results showed that *hba3* expression was not down regulated in embryos treated with succinylacetone (Figure 11B, right panel). By contrast, *Xalas2*-knockdown embryos showed significant down-regulation of *hba3* gene (Figure 11B, middle panel). Additionally, *Scl*, *Gata1*, and *Gata2* were expressed at normal levels in the succinylacetone-treated embryo (Figure 12). Although, hemoglobin

was not detected in both condition (Figure 5B, 6B and 11B). These data suggest that *hba3* expression may not be affected by heme synthesized by *Xalas2*. Abnormal function of heme as a transcription factor has been reported previously (Suragani et al 2012); however, in this study heme does not regulate α -globin expression *in vivo* (Figure 11A).

V-6. Xalas2 is required for the proliferation or/and differentiation of erythroblasts

Translational inhibition of *Xalas2* gene affected *hba3* and *Scl* expression at Stage 34 in erythroblast precursors located on VBI as I showed (Figure 7B and 8B). Finally, in order to visualize circulating erythroblasts, GFP mRNA was injected in the ventral vegetal side at the 8-cell stage and a portion of erythroblast precursors in VBI were labeled by GFP. Circulation of the enhanced green fluorescent protein (EGFP)-labeled blood cells in each conditional embryo was analyzed (Figure 13A). The number of labeled erythrocytes was low in *Xalas2* MO-injected and succinylacetone-treated embryos as compared with the control MO injected embryo. To examine the abilities of erythroblast precursors to differentiate into mature erythrocytes, circulating erythroblasts in the tadpoles were collected and their

morphology was analyzed by Giemsa staining (Figure 13B and 13C). In the control MO-injected tadpoles, characteristic small cells with nuclei were observed, similar to normal erythroblasts or basoerythrocytes. In contrast, in *Xalas2* MO-injected tadpoles showed erythroblast precursor-like morphology including trachychromatic cytoplasm and enlarged nuclei. In the tadpoles treated with succinylacetone, characteristic small cells with nuclei were observed, similar to the control MO-injected tadpoles. However, the number of blood cells was dramatically decreased, and there was no leucocytes observed in the succinylacetone-treated embryos. Additionally, the rate of immature erythroblast was about 65.5% in *Xalas2* MO-injected embryo. The value showed higher than in control MO-injected embryo and succinylacetone-treated (Figure 14). In contrast, the rate of mature erythroblast was respectively more than 63% in untreated embryo, control MO-injected and succinylacetone-treated. These data suggest that erythroblasts of *Xalas2* MO-injected and succinylacetone-treated tadpoles show characteristic differences. Thus, I concluded that heme synthesized by *Xalas2* does not regulate differentiation into erythroblast, rather *Xalas2* may independently be responsible.

VI. Discussion

Mammalian ALAS2 have been reported to be expressed specifically in erythrocytes that synthesize aminolevulinic acid as a heme mediator. Firstly, results from *Xalas2* cloning and alignment show that *Xalas2* contains 2 heme-regulatory motifs. The CP motif (Figure 1) on the pre-sequence protein, processed in the mitochondria, is widely conserved in vertebrates. These CP motifs bind to heme and prevent *alas1* processing within the mitochondria (Fukuyama et al 2007). Mitochondrial transport of mouse pre-*alas2* protein has been shown to be inhibited by addition of exogenous hemin (Lathrop and Timko 1993). *Xalas2* is thought to function similarly as mammal.

Furthermore, 5'-UTR of *alas2* contains an IRE sequence (5'-CAGUGX-3') similar to that in human, mouse, rat, and chicken (Cox et al 1991). IRE found in the transcripts that encode iron metabolism proteins is recognized by IRP (Rouault and Klausner 1997), ALAS2 is also one of the iron metabolism proteins (Cox et al 1991 and Melefors et al 1993). The 5'-UTR of the IRE transcripts form a stem-loop structure, and translation of *alas2* mRNA is inhibited in absence of iron. In contrast, in the presence of high concentration of iron, IRP does not bind to IRE, therefore *alas2* mRNA can be

translated (Hentze et al 2004). *Xalas2* is possibly regulated by iron and IRP in the embryos.

The purpose of this study was to investigate the role of *Xalas2* in erythroblast differentiation during primary hematopoiesis. *Xalas2* was specifically expressed in the anterior mesoderm, hemangioblast, and erythroblast. *Xalas2* expression during early development shows that other genes are involved in heme biosynthesis in *Xenopus laevis*. For example, it has been reported that *Alad*, *Pbgd*, *Uro3s*, and *Urod* have expressed in the egg stage (Shi et al 2008). Thus, these data suggest that *Xalas2* is a rate-limiting enzyme for heme synthesis in other vertebrates (Shi et al 2008), however *Xalas2* might have some function in hemangioblasts and pro-erythroblasts. Therefore, it is considered that *Xalas2* could be involved in the differentiation from mesoderm to hemangioblast. In *Xenopus* embryos, *Gata2* is required for hemangioblast formation by controlling *Lmo* and *Scl* (Liu et al 2008). However, *Xalas2* inhibition did not affect expression of hematopoietic transcription factor, *Scl* and *Gata2* in the hemangioblast. In contrast, *Scl* expression in VBI decreased and *hba3* expression was inhibited with injection of *Xalas2* MO in the erythroblast precursor region (Figure 7), which was not

observed with SA treatment (Figure 12). *Scl* is required for generation of erythrocyte and endothelial cells in not only hemangioblasts during primary hematopoiesis, but also in the dorsal lateral plate during definitive hematopoiesis (Mead et al 1998).

Hba3 is an α -globin gene and Hba3 protein consists of hemoglobin α subunit in the *Xenopus* larva. It is reported that α -globin transcription is regulated by heme concentration (Tahara et al 2004 and Chiabrando et al 2014). When heme biosynthesis is inactive, the transcription of α -globin is inhibited by the repressor complex of Bach1 and small Maf proteins that bind MAREs (Maf recognition elements) in the regulatory region of α -globin genes. On the other hand, when heme biosynthesis is active, heme binds Bach1 in the nucleus and mediates its export to the cytosol. Then, erythroid transcription factor, NF-E2 p45 associates with small Maf proteins and activates the transcription of globin in K562 cells (Tahara et al 2004). In this study, *hba3* expression was downregulated in *Xalas2*-knockdown embryos (Figure 11B, middle panel) but not in embryos treated with succinylacetone (Figure 11B, right panel). It is unclear why the *in vitro* and *in vivo* results differed; probably since K562, a chronic myelocytic leukemia cell line represents definitive hematopoiesis, whereas the data were obtained

with primary hematopoiesis in *Xenopus* embryos. The role of *alas2* in cytosol and the nucleus is also unknown. Thus, my data suggest a larval regulatory pathway of *hba3* transcription by *Xalas2*, which is independent of heme, Bach1 pathway, and *Gata-Scl* transcription pathway.

In zebrafish and mouse, loss of ALAS2 function caused immature erythroblast formation and the differentiation of erythroblast was delay (Beownlie et al 1998, Takahashi et al 1999). Especially, in the ALAS2 knockout mice, the present study demonstrated that low endogenous heme by loss of ALAS2 caused maturation arrest of primitive erythroid cells (Takahashi et al 1999). In this study, the *Xalas2* MO-injected tadpoles also showed characteristic erythroblast precursor-like morphology including trachychromatic cytoplasm and enlarged nuclei (Figure 13C). By contrast, in the tadpoles treated with succinylacetone, an inhibitor of heme biosynthesis, characteristic small nuclei and cells were observed, similar to the control MO-injected tadpoles. Additionally, the inhibition of heme synthesis on both of conditions caused the number of cell to decrease. Treatment of succinylacetone These data suggest that heme synthesized by *Xalas2* does not regulate differentiation into erythroblasts, rather *Xalas2*

may independently be responsible. Generally, while heme is reported to function as a transcription factor (Suragani et al 2012), it is no reports that *alas2* makes transcriptional control. In recent years, it is suggested that the C-terminal region of the mature human ALAS2 can be modified by small ubiquitin-like modifier (SUMO) molecules (Kadirvel et al 2012). SUMO protein is highly conserved from yeast to mammals (Chen et al 1998). In vertebrates, there are three major SUMO isoform (SUMO-1, SUMO-2, SUMO-3), which expressed in all tissues (Huang et al 2004). C-terminus in Glycine residue of SUMO has the region of isopeptide bond to the side chain of a particular Lys residue of the target protein (Hay 2005). *In vitro*, modification by SUMO2 and SUMO3 of actin is involved in nuclear translocation (Rosas-Acosta et al 2005). Various SUMO binding targets are reported in the cytoskeletal proteins, such as Rho family GTPase, actin and tubulin (Rosas-Acosta et al 2005 and Vertegaal AC et al 2004). Erythroblast progenitors in mouse also express adhesion proteins related cytoskeletal protein on their surface, CD44, integrins $\alpha4$, $\alpha5$, and $\beta1$ in the yolk sac (Isern et al 2011). Expressions of those were lost before entering into blood vessel. Additionally, Mouse with deletion of *mDia2*, a form in isoform and Rho effectors, fall

to form actin filaments in erythroblasts (Watanabe et al 2013 and Kalfa et al 2014).

There are no reports that these two molecules are modified by SUMO in erythroblasts.

However, from above reports, ALAS2 with cytoskeletal proteins might regulate erythroblast differentiation by the modification with SUMO in primary hematopoiesis.

In view of some possible mechanisms on mammalian, I think that XAlas2 protein might be located in cytoplasm by inhibition of transporting to mitochondria and subjected to some posttranslational modification, for example, by SUMO in this study. It might be possible that XAlas2 protein could regulate transcription of *hba3*, cell division and differentiation of erythroblast thereby.

The specific mechanism of transcriptional control by *Xalas2* is not clear.

However, in my study, the presence of a novel control mechanism of erythroid differentiation through the *Xalas2* was suggested. These results are considered to be an important finding from the view point of evolutionary diversity of the hematopoietic system.

VII. Acknowledgements

I am grateful to guidance provided by Dr. Akira Kurisaki, Associate Professor at the University of Tsukuba. I would like to thank Dr. Ito, Group Leader at National Institute of Advanced Industrial Science and Technology Drug Discovery Platform Research Department. I also thank Dr. Nakata, Dr. Hashimoto and Dr. Wang, Professor at the University of Tsukuba for many advices. I am grateful for the support provided by the National Institute of Advanced Industrial Science and Technology. I would like to thank everyone from the stem cell engineering research group. Finally, I sincerely thank my husband, Mr. Ogawa for his support.

VIII. References

1. Ajioka RS, Phillips JD, Kushner JP (2006). Biosynthesis of heme in mammals. *Biochimica et Biophysica Acta*. 1763: 723-736.
2. Baron MH, Vacaru A, Nieves J. (2013) Erythroid development in the mammalian embryo. *Blood Cells Mol Dis*. 51(4): 213-219.
3. Brownlie A, Donovan A, Pratt SJ, Paw BH, Oates AC, Brugnara C, Witkowska HE, Sassa S, Zon LI. (1998) Positional cloning of the zebrafish *sauternes* gene: a model for congenital sideroblastic anaemia. *Nat Genet*. 20(3): 244-50.
4. Chen A, Mannen H, Li SS. (1998) Characterization of mouse ubiquitin-like SMT3A and SMT3B cDNAs and gene/pseudogenes. *Biochem Mol Biol Int*. 146(6): 1161-1174.
5. Chiabrando D, Mercurio S, Tolosano E. (2014) Heme and erythropoiesis: more than a structural role. *Haematologica*. 99(6): 973-983: 10.3324/haematol.2013.091991.
6. Costa RM, Soto X, Chen Y, Zorn AM, Amaya E. (2008) *spib* is required for primitive myeloid development in *Xenopus*. *Blood*. 112(6): 2287-2296.
7. Cox TC, Bawden MJ, Martin A, May BK. (1991) Human erythroid

- 5-aminolevulinate synthase: promoter analysis and identification of an iron-responsive element in the mRNA. *EMBO J.* 10(7): 1891-1902.
8. Detrich HW 3rd, Kieran MW, Chan FY, Barone LM, Yee K, Rundstadler JA, Pratt S, Ransom D, Zon LI. (1995) Intraembryonic hematopoietic cell migration during vertebrate development. *Proc Natl Acad Sci U S A.* 92(23): 10713-10717.
 9. Furuyama K, Kaneko K, Vargas PD. (2007) Heme as a magnificent molecule with multiple missions: heme determines its own fate and governs cellular homeostasis. *Tohoku J Exp Med.* 213(1): 1-16.
 10. Goldman DC, Berg LK, Heinrich MC, Christian JL. (2006) Ectodermally derived steel/stem cell factor functions non-cell autonomously during primitive erythropoiesis in *Xenopus*. *Blood.* 107(8): 3114-3121.
 11. Haar J, Ackerman GA. (1971) A phase and electron microscopic study of vasculogenesis and erythropoiesis in the yolk sac of the mouse. *Anat Rec.* 170: 199-224.
 12. Hay RT. (2005) SUMO: a history of modification. *Mol Cell.* 18(1): 1-12.
 13. Huang WC, Ko TP, Li SS, Wang AH. (2004) Crystal structures of

- the human SUMO-2 protein at 1.6 Å and 1.2 Å resolution: implication on the functional differences of SUMO proteins. *Eur J Biochem.* 271(20): 4114-4222.
14. Harland RM. (1991) In situ hybridization: an improved whole-mount method for *Xenopus* embryos. *Methods Cell Biol.* 36: 685-695.
15. Hentze MW, Muckenthaler MU, Andrews NC. (2004) Balancing acts: molecular control of mammalian iron metabolism. *Cell.* 117(3): 285-297.
16. Isern J, He Z, Fraser ST, Nowotschin S, Ferrer-Vaquer A, Moore R, Hadjantonakis AK, Schulz V, Tuck D, Gallagher PG, Baron MH. (2011) Single-lineage transcriptome analysis reveals key regulatory pathways in primitive erythroid progenitors in the mouse embryo. *Blood.* 117(18): 4924-4934.
17. Ito Y, Kuhara S, Tashiro K. (2001) In synergy with noggin and follistatin, *Xenopus* nodal-related gene induces sonic hedgehog on notochord and floor plate. *Biochem Biophys Res Commun.* 281(3): 714-719.
18. Kadirvel S, Furuyama K, Harigae H, Kaneko K, Tamai Y, Ishida Y, Shibahara S. (2012) The carboxyl-terminal region of erythroid-specific 5-aminolevulinate

- synthase acts as an intrinsic modifier for its catalytic activity and protein stability.
Exp Hematol. 40(6): 477-486.
19. Kalfa TA, Zheng Y. (2014) Rho GTPases in erythroid maturation. Curr Opin Hematol. 2014 21(3): 165-171.
 20. Kim HY, LaVaute T, Iwai K, Klausner RD, Rouault TA. (1996) Identification of a conserved and functional iron-responsive element in the 5'UTR of mammalian mitochondrial aconitase. J Biol Chem. 271: 24226-24230.
 21. Lathrop and Timko. (1993) Regulation by heme of mitochondrial protein transport through a conserved amino acid motif. Science. 259: 522-525.
 22. Liu F, Walmsley M, Rodaway A, Patient R. (2008) Fli1 acts at the top of the transcriptional network driving blood and endothelial development. Curr Biol 18: 1234-1240.
 23. Mead PE, Kelley CM, Hahn PS, Piedad O, Zon LI. (1998) SCL specifies hematopoietic mesoderm in *Xenopus* embryos. Development. 125(14): 2611-2620.
 24. Melefors O, Goossen B, Johansson HE, Stripecke R, Gray NK, Hentze MW. (1993) Translational control of 5-aminolevulinate synthase mRNA by

iron-responsive elements in erythroid cells. *J Biol Chem.* 268: 5974-5978.

25. Nakajima O, Takahashi S, Harigae H, Furuyama K, Hayashi N, Sassa S, Yamamoto M. (1999)

Heme deficiency in erythroid lineage causes differentiation arrest and cytoplasmic iron overload. *EMBO J.* 18(22): 6282-6289.

26. Ogawa K, Sun J, Taketani S, Nakajima O, Nishitani C, Sassa S, Hayashi N, Yamamoto M, Shibahara S, Fujita H, Igarashi K. (2001)

Heme mediates derepression of Maf recognition element through direct binding to transcription repressor Bach1. *EMBO J.* 20(11): 2835-2843.

27. Palis and Yoder. (2001) Yolk-sac hematopoiesis: the first blood cells of mouse and man. *Exp Hematol.* 29(8): 927-936.

28. Palis J. (2014) Primitive and definitive erythropoiesis in mammals. *Front Physiol.* 28; 5: 3.

29. Rosas-Acosta G, Russell WK, Deyrieux A, Russell DH, Wilson VG. (2005) A universal strategy for proteomic studies of SUMO and other ubiquitin-like modifiers. *Mol Cell Proteomics.* 4(1): 56-72.

30. Shi J, Mei W, Yang J. (2008) Heme metabolism enzymes are dynamically expressed during *Xenopus* embryonic development. *Biocell*. 32(3): 259-263.
31. Sun J, Brand M, Zenke Y, Tashiro S, Groudine M, Igarashi K. (2004) Heme regulates the dynamic exchange of Bach1 and NF-E2-related factors in the Maf transcription factor network. *Proc Natl Acad Sci U S A*. 101(6): 1461-1466.
32. Suragani RN¹, Zachariah RS, Velazquez JG, Liu S, Sun CW, Townes TM, Chen JJ. (2012) Heme-regulated eIF2 α kinase activated Atf4 signaling pathway in oxidative stress and erythropoiesis. *Blood*. 119(22): 5276-5284.
33. Tashiro K, Misumi Y, Shiokawa K, Yamana K. (1983) Determination of the rate of rRNA synthesis in *Xenopus laevis* triploid embryos produced by low-temperature treatment. *J Exp Zool*. 225(3): 489-495.
34. Tober J, Koniski A, McGrath KE, Vemishetti R, Emerson R, de Mesy-Bentley KK, Waugh R, Palis J. (2007) The megakaryocyte lineage originates from hemangioblast precursors and is an integral component both of primitive and definitive hematopoiesis. *Blood*. 109: 1433-1441.

35. Tsiftoglou AS, Vizirianakis IS, Strouboulis J. (2009) Erythropoiesis: model systems, molecular regulators, and developmental programs. *IUBMB Life*. 61(8): 800-830.
36. Vertegaal AC, Ogg SC, Jaffray E, Rodriguez MS, Hay RT, Andersen JS, Mann M, Lamond AI. (2004) A proteomic study of SUMO-2 target proteins. *J Biol Chem*. 279(32): 33791-33798.
37. Wadman, I. A., Osada, H., Grutz, G. G., Agulnick, A. D., Westphal, H., Forster, A. and Rabbitts, T. H. (1997) The LIM-only protein LMO2 is a bridging molecule assembling an erythroid, DNA-binding complex which includes the TAL1, E47, GATA-1 and Ldb1/NLI proteins. *EMBO J*. 16, 3145-3157.
38. Walmsley M, Cleaver D, Patient R. (2008) Fibroblast growth factor controls the timing of Scl, Lmo2, and Runx1 expression during embryonic blood development. *Blood*. 111(3): 1157-1166.
39. Watanabe S, De Zan T, Ishizaki T, Yasuda S, Kamijo H, Yamada D, Aoki T, Kiyonari H, Kaneko H, Shimizu R, Yamamoto M, Goshima G, Narumiya S.

(2013) Loss of a Rho-Regulated Actin Nucleator, mDia2, Impairs Cytokinesis during Mouse Fetal Erythropoiesis. *Cell Rep.* 5: 926–932.

40. Wilber A, Nienhuis AW, Persons DA. (2011)

Transcriptional regulation of fetal to adult hemoglobin switching: new therapeutic opportunities. *Blood.* 117(15): 3945-3953.

IX. Figures and Legends

Figure 1. Alignment of Alas2 protein sequences of *Xenopus* (type A accession no. NP_001087499; type B accession no. AAH84616), human (accession no. NP_000023), mouse (accession no NP_033783), and zebrafish (accession no NP_571757). The yellow box indicates the heme regulatory motif (CP motif [Arg, Lys or Asn]-Cys-Pro-[Lys or hydrophobic residue]-[Lue or Met]). The blue box indicates the catalytic core domain. The green arrowhead indicates the site of precursor protein processing by mitochondrial peptidase. Amino acids indicated in red are conserved amino acid in *Xenopus*, human, mouse, and zebrafish.

Figure 2. *Xalas2* and erythrocyte-related gene expression in *X. laevis* embryos. (A) RT-PCR analysis of *Xalas2* type a and b expression during *Xenopus* development. Ornithine decarboxylase (*odc*) served as an internal control. Whole-mount *in situ* hybridization analysis using *Xalas2* antisense probe (B–F, D'–F', E', F''), *hba3* (G–J, I', J'), and *Scl* (K–N). (B) Stage 15: ventral view shows weak *Xalas2* expression in the

anterior mesoderm (arrowhead). (C) Stage 18: expression in the anterior mesoderm (arrowhead) is extensive, as viewed from the ventral side. (D, D') Stage 23, (E, E') stage 34: ventral, lateral views of the same embryo show extensive staining in the hemangioblast and ventral blood island (VBI) (arrows). (F, F') Stage 38: expression of *alas2* is distinct in the circulatory system (ventral and lateral views). Eosin-stained sections showing *Xalas2* expression in stage 34 (E'') and stage 38 (F'') and *hba3* in the same stages (I', J'). Transverse sections of embryos on the red lines in panels E'', F'', I', J' are shown in panels E', F', I', J'. Scale bars in stages 15, 18, and 23 represent 0.5 mm; in Stages 34 and 38, 0.1 mm.

Figure 4. (A) *Xalas2*-MO was designed to target the sequence around the translational start codon of both *Xalas2* alleles (*Xalas2a* and *Xalas2b*). *Xalas2a*-MO/5mis and *Xalas2b*-MO/5mis have five mutations and serve as the negative control. Identical residues are indicated in red. (B) Western blot analysis of c-Myc-tagged XAlas2 proteins in the embryos co-injected with the indicated mRNAs and MO. Actin was used as the internal control. Both alleles were targeted by *Xalas2a* MO and *Xalas2b* MO

(lane 2, 8). *Xalas2a* MO and *Xalas2b* MO/5mis failed to target these genes (lanes 5, 11).

Figure 3. Region-specific translational inhibition of *Xalas2* gene by the injection of red-gal and *Xalas2* MO. Whole-mount *in situ* hybridization of *Xalas2* and Red-gal staining were performed. (A) Upon dorsal vegetal injection, *Xalas2* translation was inhibited in hemangioblasts at St23 (upper). (B) Upon ventral vegetal injection, *Xalas2* translation was inhibited in the ventral blood island at St34 (lower panel).

Figure 5. Hemoglobin staining in *Xalas2* MO-injected embryos and the control MO-injected embryos at Stage 42. (A) Schematic pathway of heme synthesis and inhibition of *Xalas2* translation. These MOs were injected into (B) dorsal vegetal and (C) ventral vegetal in 8-cell stage. The red regions in the cartoon indicate the tissue where translation of *Xalas2* was inhibited at Stage 23 and Stage 34. The figures on the lower line are enlarged pictures around the heart. Scale bars on upper line and lower line were 0.5 mm and 0.25 mm, respectively.

Figure 6. (A) Schematic of the heme synthesis pathway and inhibition of ALAD with succinylacetone. (B) Staining of hemoglobin in the embryos treated with succinylacetone at the indicated concentrations from the 8-cell-stage to Stage 42.

Figures on upper panel show the picture of the head and body. The enlarged figure of the heart is shown on the lower panel. Scale bars in upper and lower figures are 0.5 mm and 0.25 mm, respectively.

Figure 7. Expression of hematopoietic transcription factor in *Xalas2* MO injected embryo. Embryos were microinjected with 40 ng of *Xalas2* MO in the dorsal-vegetal side (A) and the ventral-vegetal side (B). Red colored region indicates the location of *Xalas2* MO injected with either dorsal-vegetal side or ventral-vegetal side at 8-cell Stage. Whole-mount *in situ* hybridization of *scl* in Stages 23 and 34 (A and B), of *Gata2* in Stage 23, and of *Gata1* in Stage 34 (B) are shown. The block arrow indicates two crossing lines in *scl* expression in control MO-injected embryo. The red arrow indicates decrease in *scl* expression in *Xalas2* MO-injected embryo. The number of representative phenotypes among total number of injected embryos is shown at the left bottom corner

of each figure. The experiments were performed independently at least twice. Scale bars represent 0.5 mm.

Figure 8. The expression of *hba3* in *Xalas2* MO-injected embryos. Embryos were microinjected with 40 ng *Xalas2*-MO in the dorsal-vegetal side (A) or the vegetal side (B). Whole-mount *in situ* hybridization of *hba3* at Stages 23 and 34 are shown. The arrows indicate the loss of *hba3* expression. The number of phenotypes among total number of injected embryos is shown at the lower left bottom corner of each figure. The experiments were performed independently more than three times. Scale bars represent 0.5 mm.

Figure 9. The *hba3* expression was semi-quantitated in the embryo injected with control MO- or *Xalas2* into dorsal vegetal side (A), ventral vegetal side (B). (A) Embryos expressing *hba3* maintained the V-shape region (arrow) in VBI, designated as (+), and reduced embryos were counted as (-); “Other” represents an abnormal phenotype with *hba3* expression. (B) Maintained expression of *hba3* in the control

embryo in the whole posterior region was counted as (+). The expression observed in the posterior-and-midline VBI was counted as (+/-), and the expression in the anterior VBI was counted as (-). (C) *Hba3* expression was semi-quantitated in the control MO- and *Xalas2* MO-injected embryos into ventral vegetal side. The experiments were performed in three independent replicates. Student's t-test was used to determine significant differences. $P < 0.05$ was taken as statistically significant. Scale bars represent 0.5 mm.

Figure 10. Rescue of *hba3* in *Xalas2* MO-injected embryos by co-injecting MO-insensitive *Xalas2a/5mis* mRNA. (A) *Xalas2a/5mis* was designed with 5 point mutations. (B) Knockdown of *Xalas2* caused low-level *hba3* expression on VBI; this effect was reversed by co-expression of 1 ng of *Xalas2a/5mis* mRNA. *Hba3* expression was rescued in the posterior (+) and midline VBI (+/-); (-), not rescued. Scale bars represent 0.5 mm.

Figure 11. Regulation of α -globin transcription by heme biosynthesis. (A) Inhibition of ALAD by competitive substrate, succinylacetone. Heme-dependent α -globin transcription reported by Tahara et al 2004 and Ogawa et al 2001. (B) Hemoglobin staining and *hba3* expression in *Xalas2* knock-down or succinylacetone treatment at Stage 34. The arrowhead indicates hemoglobin staining. All scale bars indicate 0.5 mm.

Figure 12. Expression of hematopoietic transcription factor in the embryos treated with succinylacetone (SA) of 0.25 mM from the 8-cell-stage to Stage 34. Whole-mount *in situ* hybridization of *scl* and *Gata2* in Stage 23 and of *Gata1*, *hba3*, and *Scl* in Stage 34 are shown. Scale bars represent 0.5 mm.

Figure 13. *Xalas2* is essential for the development of mature erythroblasts. (A) Circulating EGFP-labeled erythroblasts in the embryos either injected with the control-MO or *Xalas2*-MO or treated by succinylacetone. (B) Representative morphology of blood cells stained by Giemsa. The blood cells were harvested from embryos at Stage 42. The arrowheads indicate circulating erythroblasts. (C) Enlarged views in each condition.

Figure 14. The morphological difference in erythroblast after inhibition of heme biosynthesis. The representative morphology of blood cells stained by Giemsa. The blood cells were harvested from embryos at Stage 42. The cells are represented as cells observed in 58mm². Scale bars represent 0.5 μ m.

Kalae2a	MASLIINRCPFATREDPTVFLRVANPFLINSAERCPIMVTRSLSTSGAGEORAKDIPPAATGVSTGASNRKTLAQAPQAALANATCPFIENEIGKEGGSIVQRAAGPQVQEDISAFKTDALSS	120
Kalae2b	MASLIINRCPFATREDPTVFLRVANPFLINSAERCPIMVTRSLSTSGAGEORAKDIPPAATGVSTGASNRKTLAQAPQAALANATCPFIENEIGKEGGSIVQRAAGPQVQEDISAFKTDALSS	111
ALAS2 (human)	-----MVTAMMLIQCCPVLARGPNSILGKVVTKHQFLFGIGRCPIIATQGNCSQIHLKATKAGGDSPSWAKGCPFMJSELQDGKSIYOKAAPEVQEDVKARKTD-LPS	105
ALAS2 (mouse)	-----MVAAMLLNSCPVLJSGPPTGLLGVAKTYQFLFSIGRCPIIATQGPPTCSQIHLKATKAGGDSPSWAKSHCPFMJSELQDRKSIYQRAAPEVQEDVKARKTD-LIS	105
ALAS2 (zebrafish)	-----MSAFIHHICPFLISSPSPSARKATYIYLNADRCPIIYVQISAKAAGSSQNGLLPHKPKKQALATTAQVAVSMSQSCPFSVKIGLVKASIPQVQ	94
Kalae2a	LLIEVOSSLKKKFLTPSSKKVNIQTGAPLIPTHLIKENISGRAAFGYDDFSSRIIEKKSDHTEYRVFKTVNRRADAYPPAEEDYSDLHGEKKEVSVVWCSDNYLQMSRHRPVLKAISEALQE	240
Kalae2b	LLIEVOSSLKKKFLTPSSKKVNIQTGAPLIPTHLIKENMTGKT-FGYDDFSSRIIEKKSDHTEYRVFKTVNRRADAYPPAEEDYSDLHGEKKEVSVVWCSDNYLQMSRHRPVLKAISEALQE	230
ALAS2 (human)	SLYSV--SLRKKP--SGPQEQEISGK---VTHLIQNNMPTGNVYFSYQGFRAKIMEKKQDHHYRVFKTVNRRADAYPPAQHFSSEAVSASKDVSVMCSDNYLQMSRHRPVLQVQETLQRTQR	218
ALAS2 (mouse)	TMDST--TRSHSP--PSFQEPQETEGA---VPHLIQNNMTGSAFGYDQFRAKIMEKKQDHHYRVFKTVNRRANAYPPAQHFSSEASVASKDVSVMCSDNYLQMSRHRPVLQAIETLQKN	218
ALAS2 (zebrafish)	EDVQPNLENQDISEGLISSLFSGLQSHQSTGPTHLIQDNFN-RPTFSYDEFFIQKIVEKKKDHTEYRIFKTVNRRAEVFPFAEDYSIAGHLGSGQVSVWCSDNYLQMSRHRPVLKAIGDALKK	213
Kalae2a	HGAGAGGTRNISGTSKXYHVDLECELADLHNKDAALLFSSCFVANDSALEFTLAKMLPGCEIYSDAGNHASMIQGI RNSGVTKVFRHNDPAHLBELLOKADKTPKIVAFETVHSMDDGALIC	360
Kalae2b	HGAGAGGTRNISGTSKXYHVDLECELADLHNKDAALLFSSCFVANDSALEFTLAKMLPGCEIYSDAGNHASMIQGI RNSGVTKVFRHNDPAHLBELLOKADKTPKIVAFETVHSMDDGALIC	350
ALAS2 (human)	HGAGAGGTRNISGTSKXYHVDLECELADLHNKDAALLFSSCFVANDSALEFTLAKMLPGCEIYSDAGNHASMIQGI RNSGVTKVFRHNDPAHLBELLOKADKTPKIVAFETVHSMDDGALIC	338
ALAS2 (mouse)	HGAGAGGTRNISGTSKXYHVDLECELADLHNKDAALLFSSCFVANDSALEFTLAKMLPGCEIYSDAGNHASMIQGI RNSGVTKVFRHNDPAHLBELLOKADKTPKIVAFETVHSMDDGALIC	338
ALAS2 (zebrafish)	HGAGAGGTRNISGTSKXYHVALENELARLHQKDGALVFSSCFVANDSALEFTLAKMLPGCEIYSDAGNHASMIQGI RNSGVTKVFRHNDPAHLBELLOKADKTPKIVAFETVHSMDDGALIC	333
Kalae2a	PLEEMCDVAHKYGAALTFVDEVHVAVGLYGTHTGAGVGERDGMHMDIISGTLGKAFGCYGGYIASTASLIDTVSYAAGFIPTTSLPPMVLAGAIVESVVLKSEGGALRRARHQRNVKMMR	480
Kalae2b	PLEEMCDVAHKYGAALTFVDEVHVAVGLYGTHTGAGVGERDGMHMDIISGTLGKAFGCYGGYIASTASLIDTVSYAAGFIPTTSLPPMVLAGAIVESVVLKSEGGALRRARHQRNVKMMR	470
ALAS2 (human)	PLEELCDVSHQYGALTFVDEVHVAVGLYGSRRGAGIGERDGMHMDIISGTLGKAFGCYGGYIASTASLIDTVSYAAGFIPTTSLPPMVLGALLESVRLKSEGGALRRARHQRNVKMMR	458
ALAS2 (mouse)	PLEELCDVAHQYGALTFVDEVHVAVGLYGARGAGIGERDGMHMDIISGTLGKAFGCYGGYIASTASLIDTVSYAAGFIPTTSLPPMVLGALLESVRLKSEGGALRRARHQRNVKMMR	458
ALAS2 (zebrafish)	PLEELCDVAHKYGAALTFVDEVHVAVGLYGAHAGCVGERDGMHMDIISGTLGKAFGCYGGYIASTASLIDTVSYAAGFIPTTSLPPMVLGALLESVRLKSEGGALRRARHQRNVKMMR	453
Kalae2a	QILLMDAGLPVINCPSHSIPIRVGNNAINSRICDVLISQNIYVQAINVPTVPBGEELLRLAPSPHHPTDMNTYFVESVVSAMKEVGMPLHTPSAAECNFCRDLHFDLMSIEWERTYFGNM	600
Kalae2b	QILLMDAGLPVINCPSHSIPIRVGNNAINSRICDVLISQNIYVQAINVPTVPBGEELLRLAPSPHHPTDMNTYFVESVVSAMKEVGMPLHTPSAAECNFCRDLHFDLMSIEWERTYFGNM	590
ALAS2 (human)	QILLMDRGRPVIPCPSHSIPIRVGNNAALSKLCDLLSKHGIIYVQAINVPTVPBGEELLRLAPSPHHSQMMEDFVEKILLAVAVGLPLQDVSVAAACNFCRDLVHFEIEMSEWERSYFQNM	578
ALAS2 (mouse)	QILLMDRGRPVIPCPSHSIPIRVGNNAALNSKICDILLSKHSIYVQAINVPTVPBGEELLRLAPSPHHSQMMENFVEKILLAVEVGLPLQDVSVAAACNFCRDLVHFEIEMSEWERSYFQNM	578
ALAS2 (zebrafish)	QILLMDAGLPVINCPSHSIPIRVGNNAAKNSEVCDILLEKHNIYVQAINVPTVPBGEELLRLAPSPHNPIMMNYFAEKILLDVQEVGLPLNGPAQASCFCDRLHFDLMSIEWERSYFQNM	573
Kalae2a	EPKYITMYA-	609
Kalae2b	EPKYITMYA-	599
ALAS2 (human)	GPQYVTTYA-	587
ALAS2 (mouse)	GPQYVTTYA-	587
ALAS2 (zebrafish)	EPRYITVAAG	583

Figure 1.

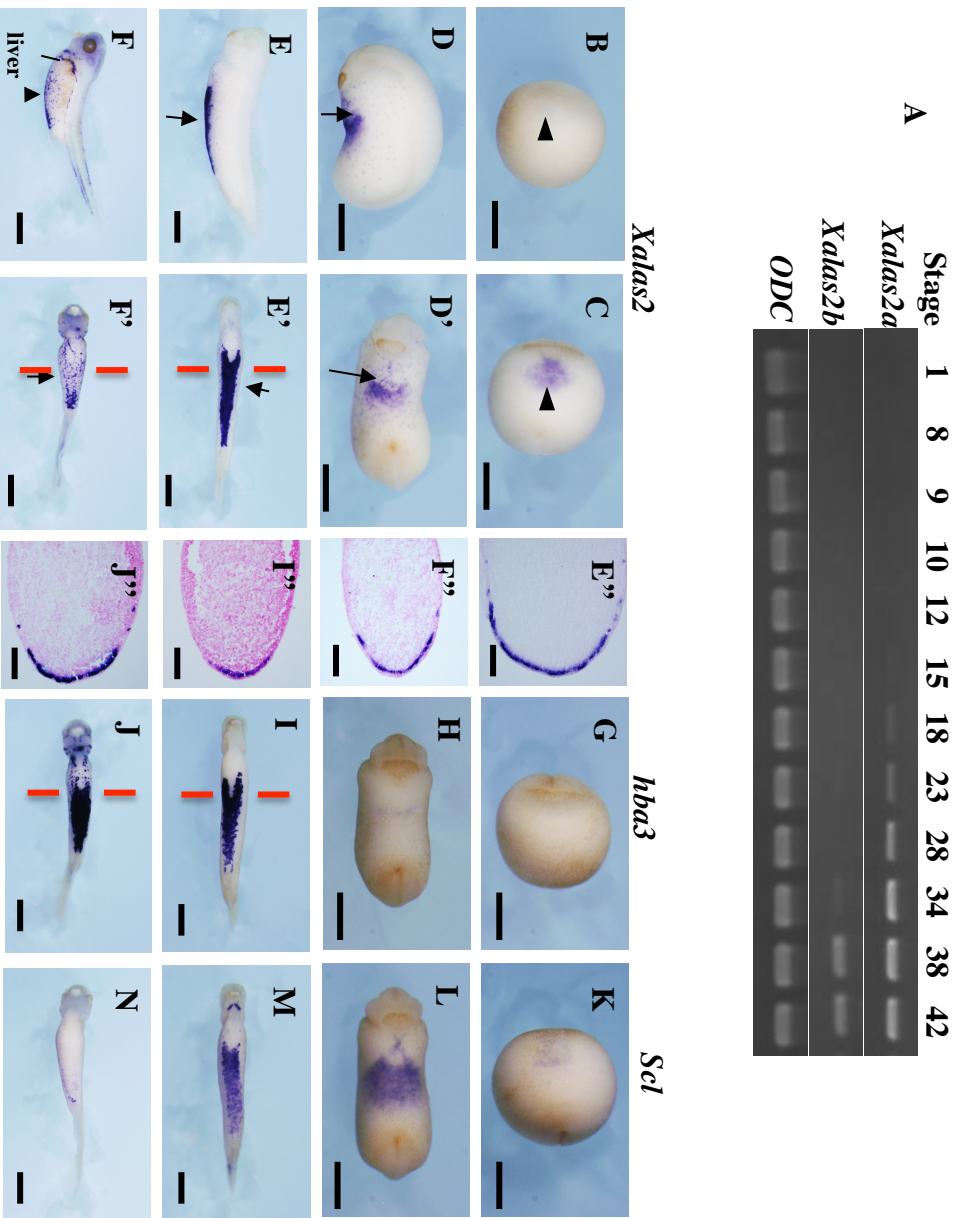
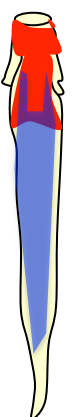
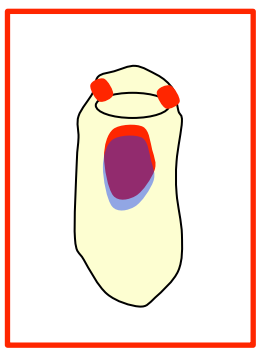
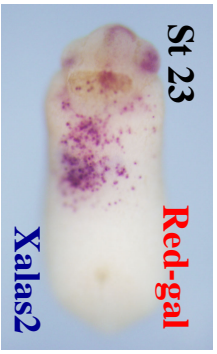
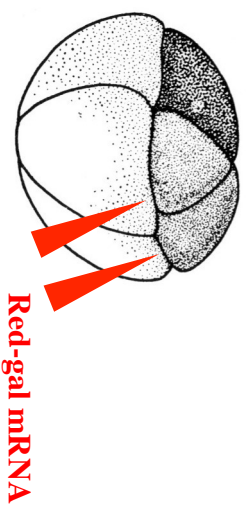


Figure 2.

A: dorsal vegetal injection



B: ventral vegetal injection

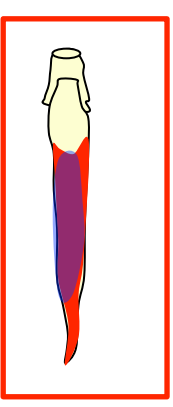
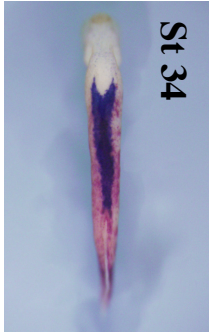
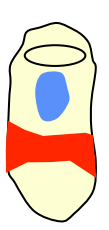
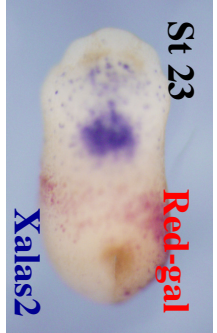
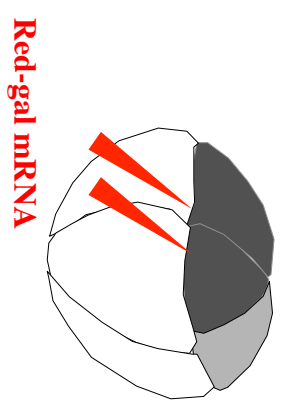


Figure 3.

A

Xalas2a -34..CAGTGCAGGGCAAC-----AGAAACCCTGACCGTGTGAACATGGCTTCTCTCATTTAATCGTTGTCCTT..+29
Xalas2a MO GAACATGGCTTCTCTCATTTAATCGT
Xalas2a/5mis CATGGCATCACTGATAAATCGAATGTCCCTT

Xalas2b -34..CAGTGCAGGGCAAC----AGACACCCTTGACGTGTGAACAATGGCTTCTCTCATCAATCGTTGTCCCTA..+29
Xalas2b MO ACATGGCTTCTCTCATCAATCGTTG
Xalas2b/5mis CATGGCATCACTGATAAATCGAATGTCCCTA

B

	1	2	3	4	5	6	7	8	9	10	11	12
5' <i>Xalas2a</i> -MTT	+	+	-	-	-	-	5' <i>Xalas2b</i> -MTT	+	+	-	-	-
<i>Xalas2a/5mis</i> -MTT	-	-	-	+	+	-	<i>Xalas2b/5mis</i> -MTT	-	-	-	+	+
<i>Xalas2a</i> MO	-	+	-	-	+	-	<i>Xalas2b</i> MO	-	+	-	+	-

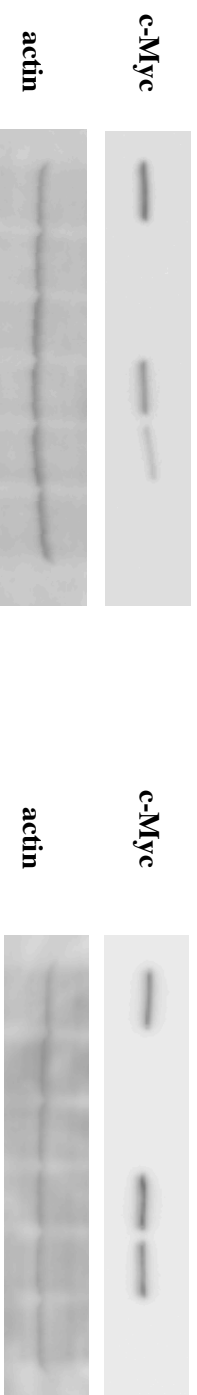


Figure 4.

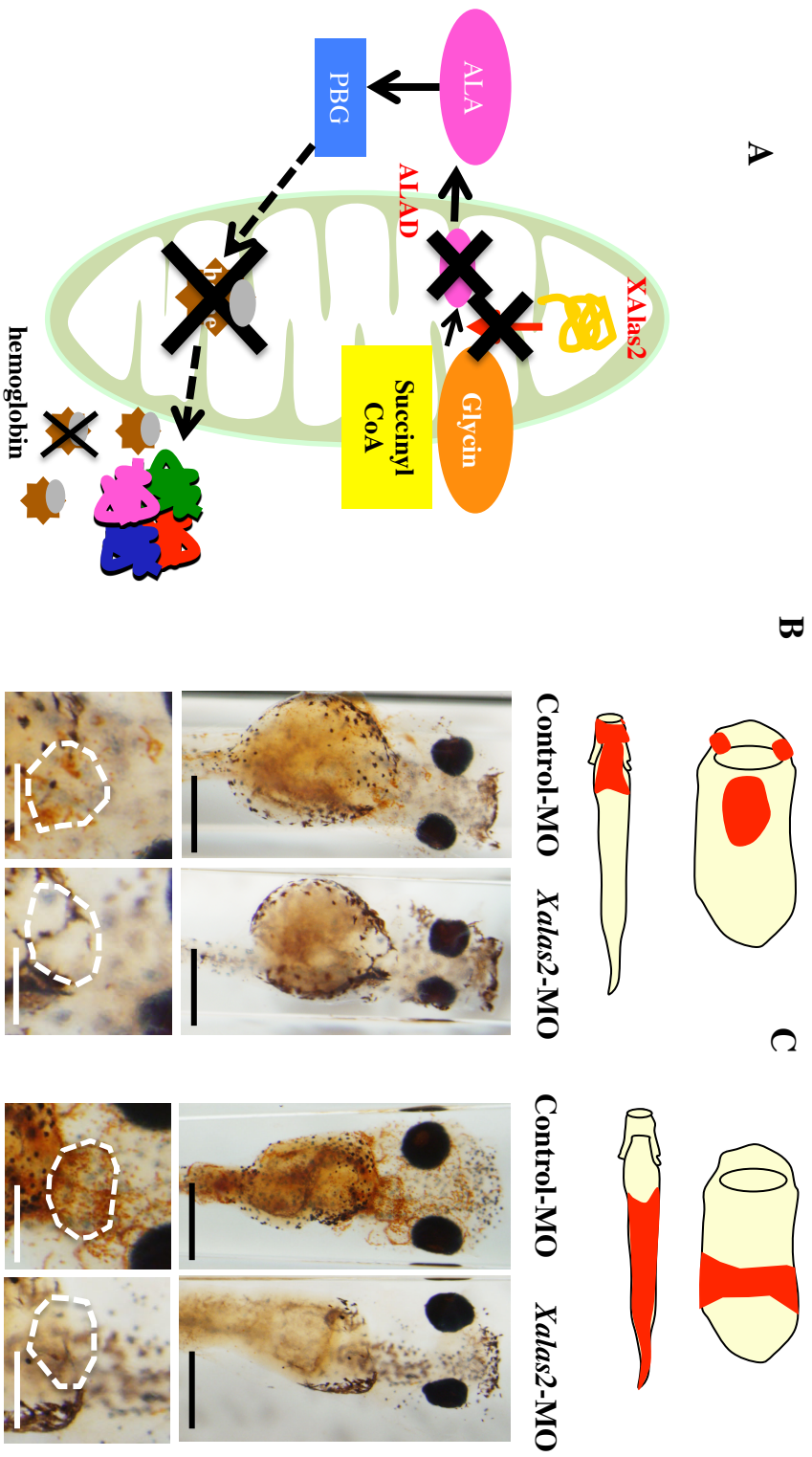


Figure 5.

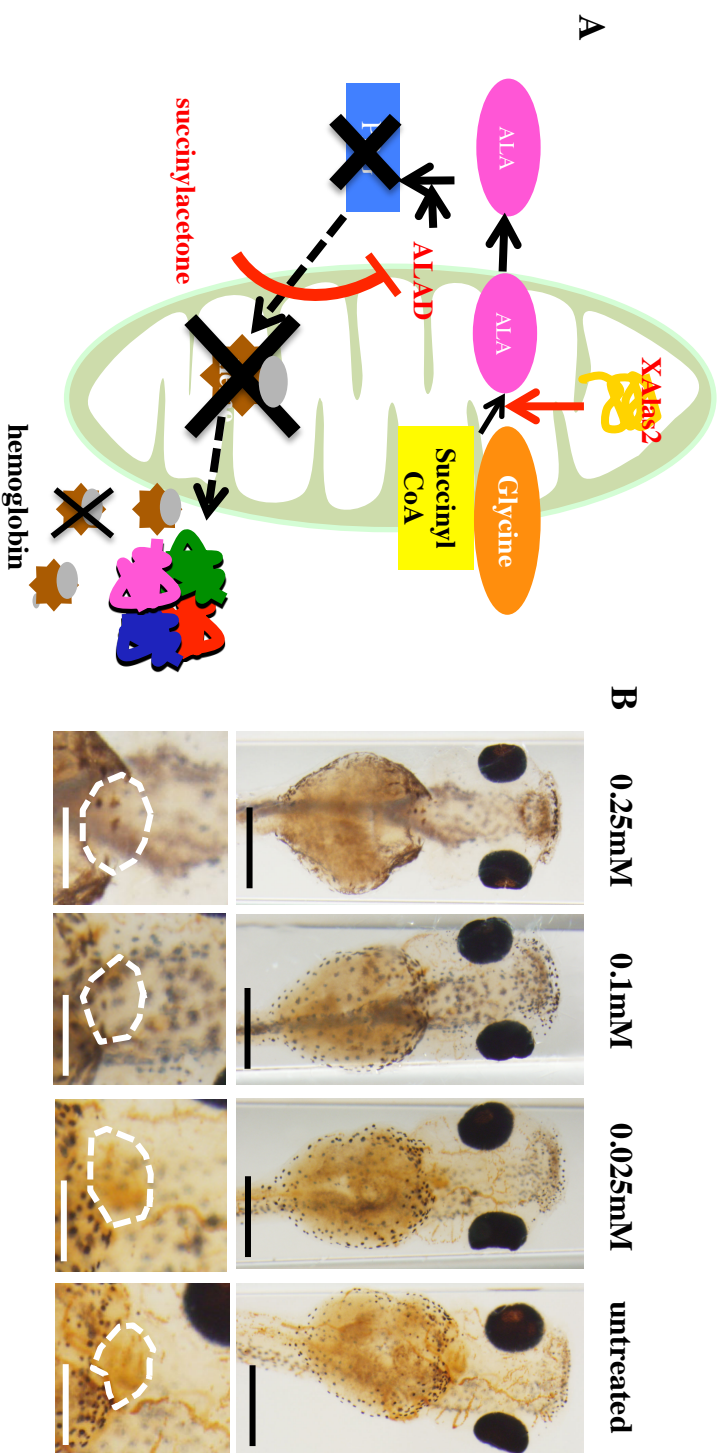
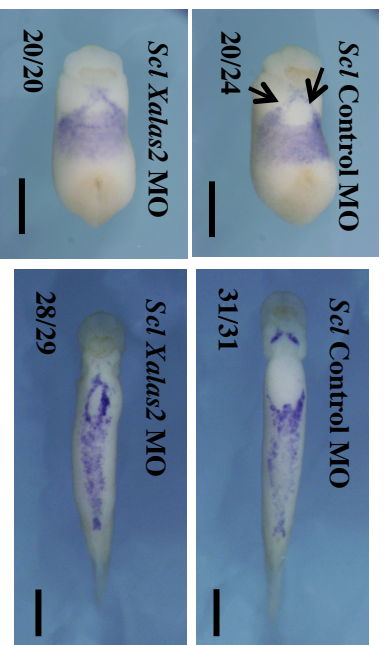
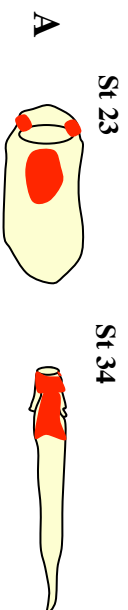


Figure 6.

***Xalas2*-MO injected into dorsal-vegetal side at 8 cell Stage**



***Xalas2*-MO injected into ventral-vegetal side at 8 cell Stage**

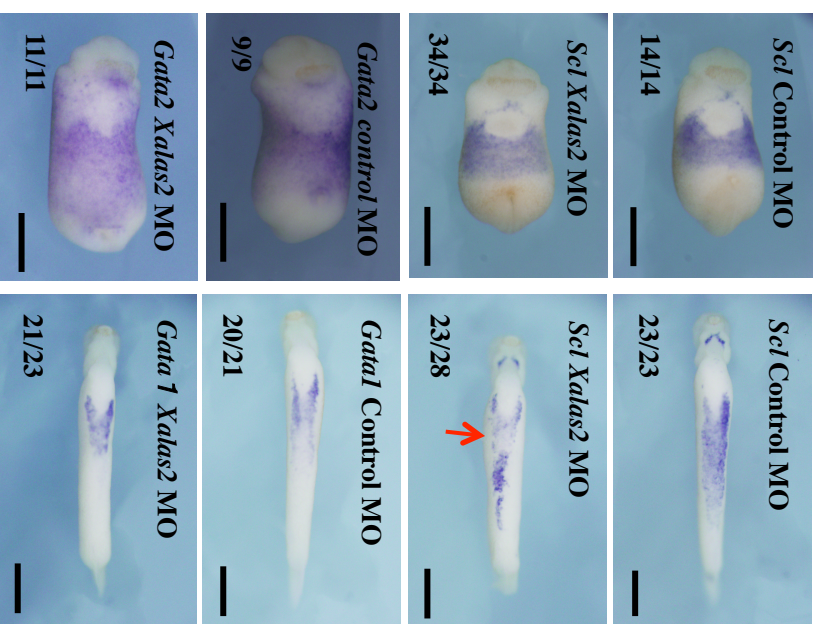
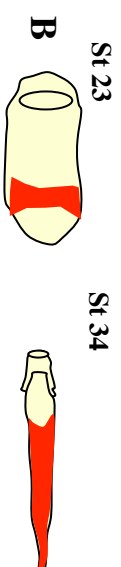


Figure 7.

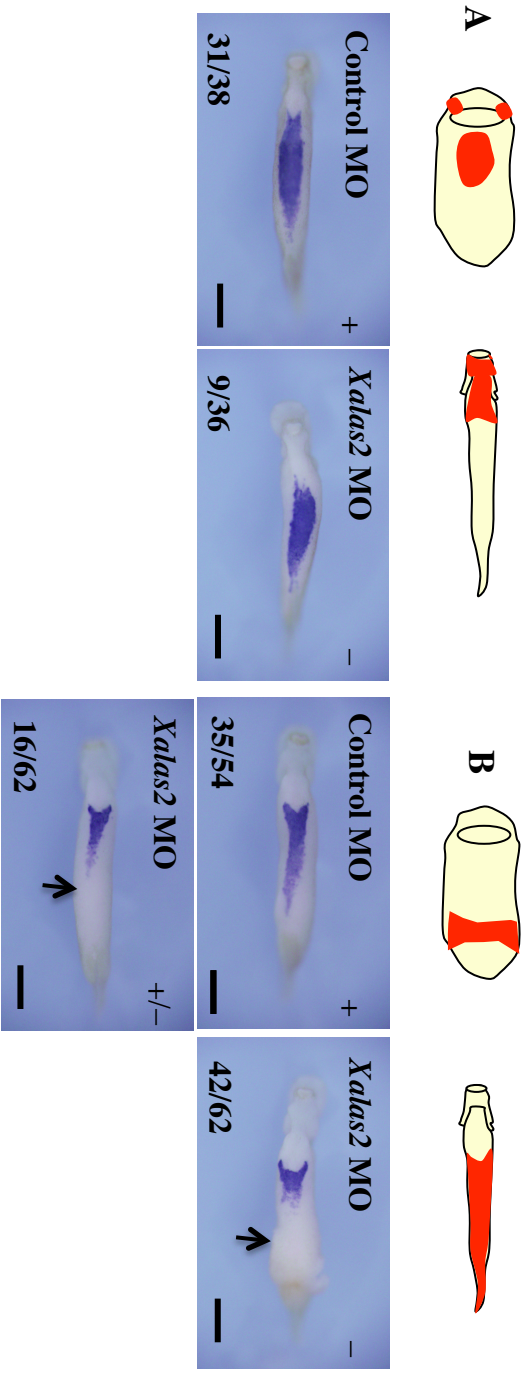
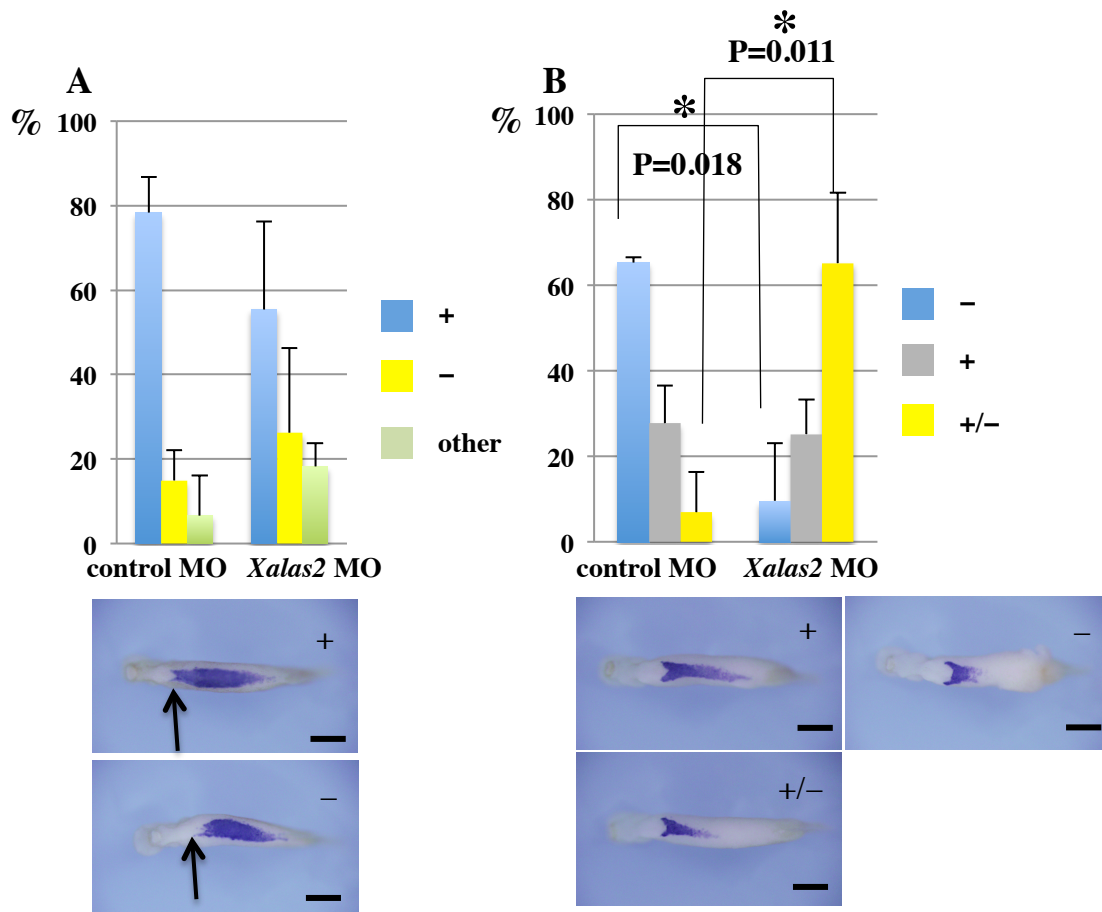


Figure 8.



C Control MO-injected embryo

***Xalas2* MO-injected embryo**

	+	+/-	-	total		+	+/-	-	total
1	4(66%)	2(33%)	0	6	1	3(25%)	3(33%)	6(62%)	12
2	20(64%)	10(32%)	1(3%)	31	2	1(3%)	9(33%)	17(62%)	27
3	11(64%)	3(17%)	3(17%)	17	3	0	4(17%)	19(82%)	23
total	35(64%)	15(27%)	4(6%)	54	total	4(9%)	16(27%)	42(68%)	62

Figure 9.

A

Xalas2a -9.. CGTGT**GAACATGGCTTCTCTCATTAATCGT**TGTC CCTT..+29
Xalas2a-MO **GAACATGGCTTCTCTCATTAATCGT**
Xalas2b -20..CGTGTGA**ACATGGCTTCTCTCATCAATCGTTG**TCCCTA..+29
Xalas2b-MO **ACATGGCTTCTCTCATCAATCGTTG**
Xalas2a/5mis **CATGGC**ATCACTGATAAATCGATG**TCCCTT**

B

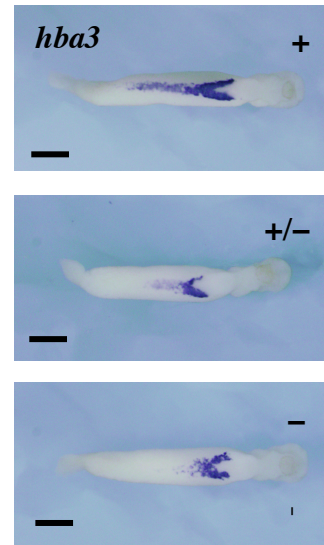
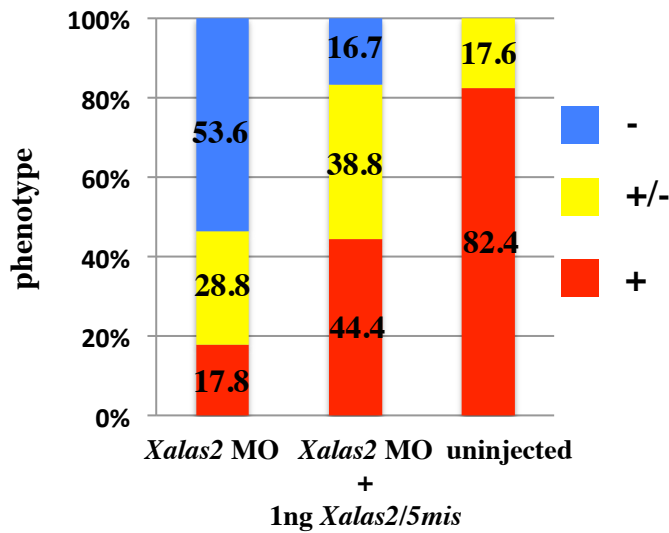
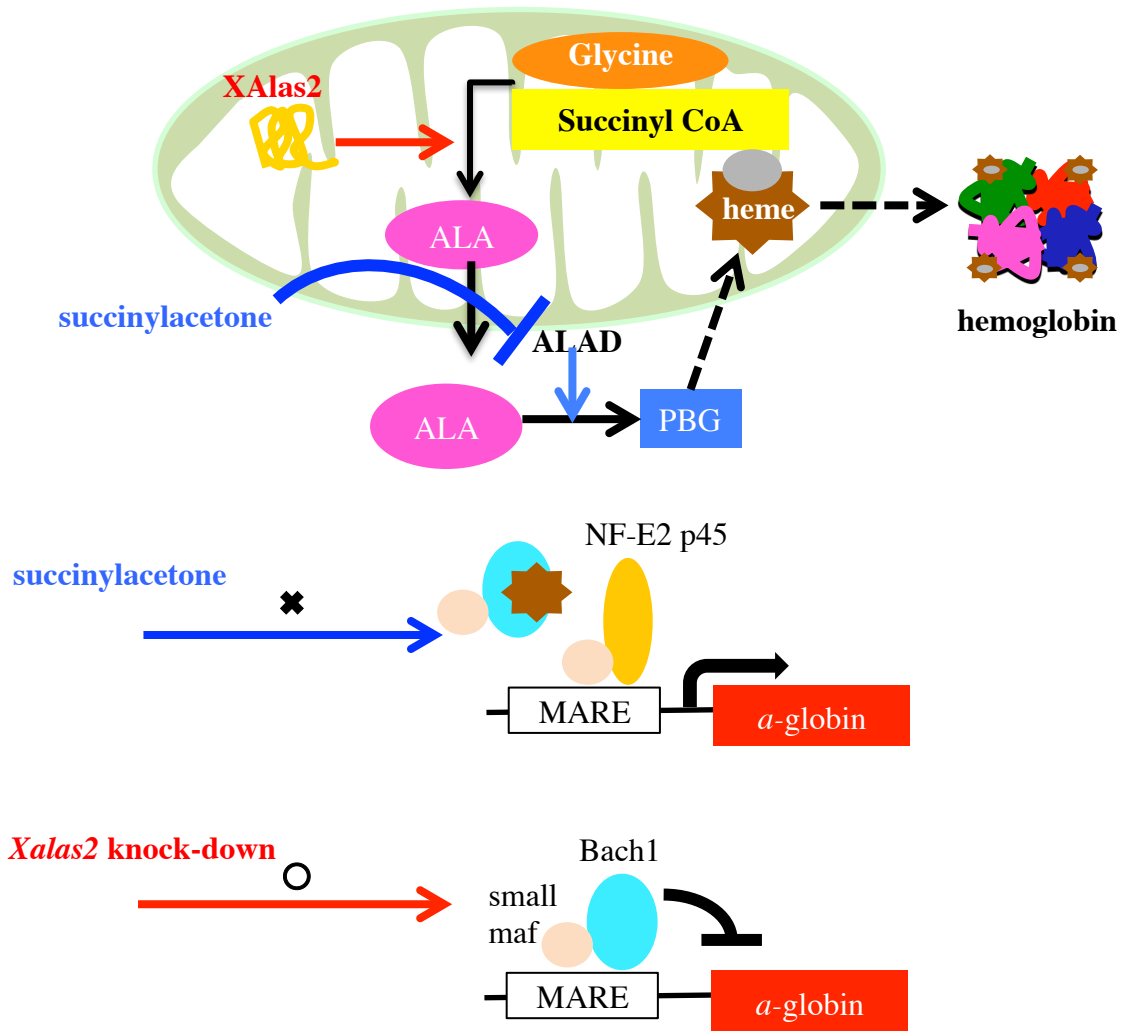


Figure 10.

A



B

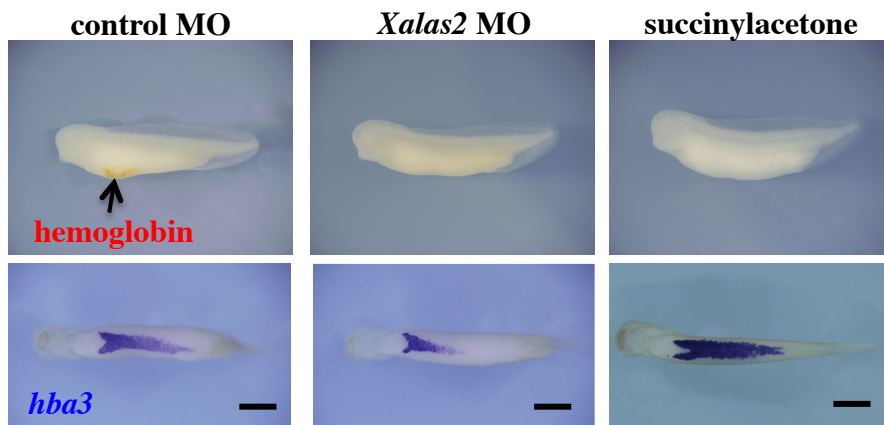


Figure 11.

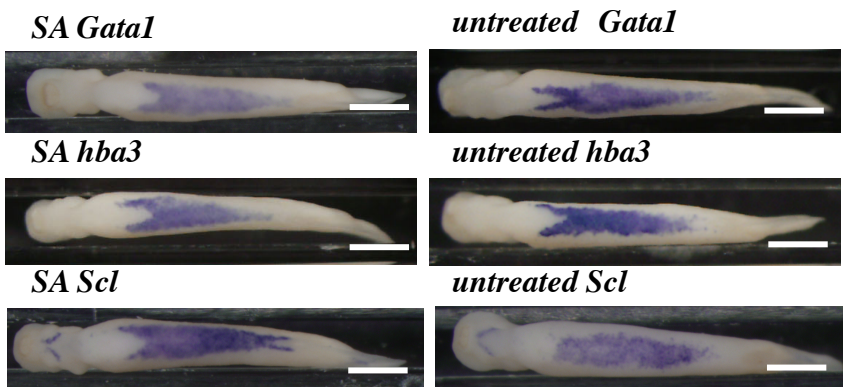
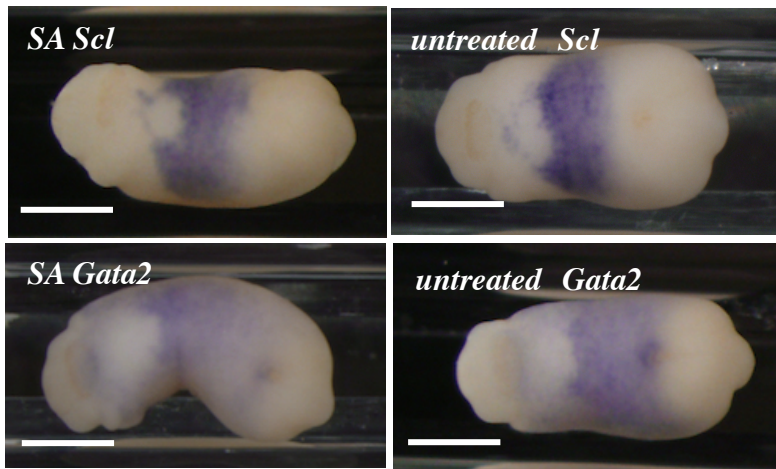


Figure 12.

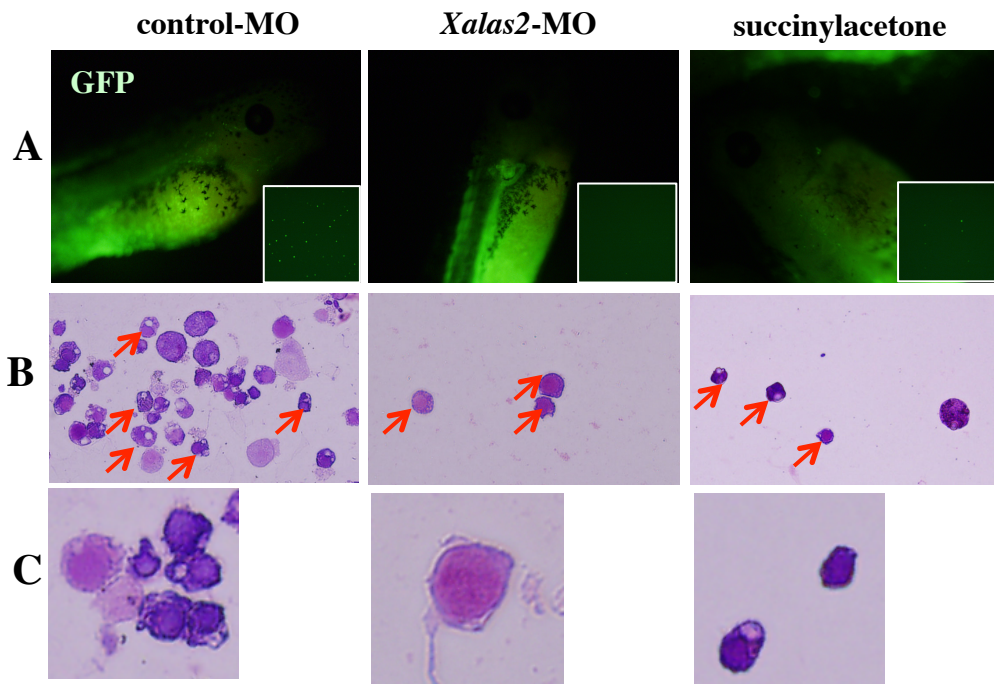
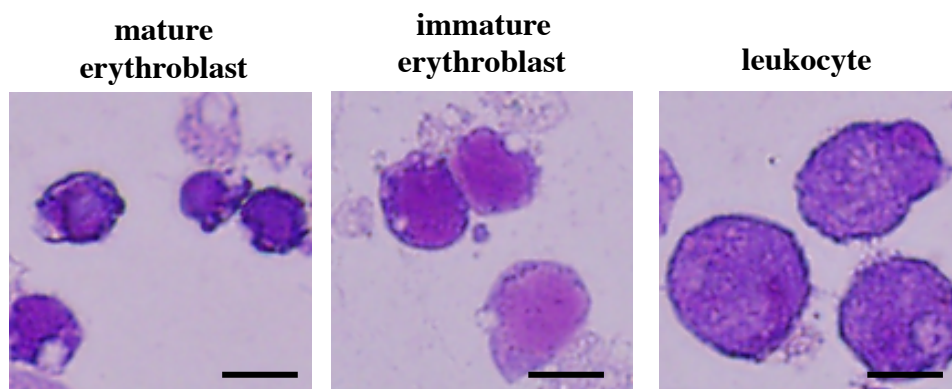


Figure 13.



	mature erythroblast	immature erythroblast	leukocyte
untreated	63.7±8.4 %	33.1±8.3 %	3.0±0.6 %
control MO	73.9±7.8 %	21.4±8.6%	4.6±1.3%
<i>Xalas2</i> MO	28.5±4.5 %	65.5±3.5 %	5.8±0%
SA	91.1±8.3%	0%	8.8±8.3%

Figure 14.